AIAA 80-0134R

Predictions of Channel and Boundary-Layer Flows with a Low-Reynolds-Number Turbulence Model

Kuei-Yuan Chien*
Naval Surface Weapons Center, Silver Spring, Md.

A new turbulence model that is valid down to the solid wall has been developed. Although the general approach is similar to that of Jones and Launder, the detailed proposals are quite different. The Taylor series expansion technique has been used to systematically study the proper behavior of the turbulent shear stress and the kinetic energy and its rate of dissipation near a solid wall. The model was applied to the problem of a fully developed turbulent channel flow and to a turbulent boundary-layer flow over a flat plate. Results were compared with the model of Jones and Launder and with various experimental data. For the cases considered, the present model compares well with the measurements and yields better predictions of the peak turbulent kinetic energy than the model of Jones and Launder.

Introduction

BECAUSE of the recent tremendous increase in the capability of digital computers, it has become possible to model the turbulent processes using transport equations derived from the Navier-Stokes equation. Since there are more unknowns than the number of equations available, this so-called closure problem has been handled with different degrees of sophistication by various research groups (see, e.g., Ref. 1). The most popular class includes the two-equation models in which two partial differential equations are used to describe the development of the turbulent kinetic energy and of a quantity related to the turbulence length scale.[2-5] However, the effects of the kinematic viscosity on the turbulence structure were ignored in many of these treatments. Consequently, the exact boundary conditions at the wall cannot be used when the turbulence Reynolds number is not high as, e.g., in flows with rapid expansions or near the transition/turbulence interface.

The general goal of the present investigation was to develop a single transport model from the Navier-Stokes equation for accurate predictions of skin friction, heat transfer, and fluctuating kinetic energy distributions in transitional and turbulent flow regimes. As a first step toward this general goal, a new turbulence model valid down to the solid wall is formulated in this paper. Turbulence model equations which provide predictions of the flow within the viscous layer adjacent to the wall have been proposed by several investigators.[3,4,6,7] Although the general approach of the present model is the same as that of Jones and Launder,[3] the detailed proposals are substantially different. In the present study, the Taylor series expansion technique was used to systematically investigate the proper behavior of the turbulent shear stress and the kinetic energy and its rate of dissipation near a solid wall. The results were used in developing a new turbulence model which retains the proper physical behavior of the balance between the dissipation and the molecular diffusion of the turbulent kinetic energy at the solid wall. The model was applied to the problems of a fully developed turbulent channel flow and of a turbulent boundary-layer flow over a flat plate. Results on skin friction, the distribution of mean velocity, turbulent shear stress, and turbulent kinetic energy will be presented and compared with available experimental data and with the theory of Jones and Launder.

Presented as Paper 80-0134 at the AIAA 18th Aerospace Sciences Meeting, Pasadena, Calif., Jan. 14-16, 1980; submitted Jan. 16, 1980; revision received July 21, 1981. This paper is declared a work of the U. S. Government and therefore is in the public domain.

*Research Aerospace Engineer, Applied Mathematics Branch. Associate Fellow AIAA.

The Turbulence Model

The limiting form of the present model in regions where the direct effect of viscosity on the turbulence structure is negligible is the same as that of Jones and Launder[3]

$$\frac{Dk}{Dt} = \frac{\partial}{\partial y}\left(\nu_t \frac{\partial k}{\partial y}\right) + \nu_t\left(\frac{\partial u}{\partial y}\right)^2 - \epsilon \tag{1}$$

$$\frac{D\epsilon}{Dt} = \frac{\partial}{\partial y}\left(\frac{\nu_t}{\sigma}\frac{\partial \epsilon}{\partial y}\right) + c_1 \frac{\epsilon}{k}\nu_t\left(\frac{\partial u}{\partial y}\right)^2 - c_2\frac{\epsilon^2}{k} \tag{2}$$

and

$$-\overline{u'v'} = \nu_t \frac{\partial u}{\partial y} \tag{3}$$

The turbulent (or eddy) viscosity is given by

$$\nu_t = c_\mu \frac{k^2}{\epsilon} \tag{4}$$

where $c_\mu = 0.09$, $c_1 = 1.35$, $c_2 = 1.8$, and $\sigma = 1.3$. The values of c_1 and c_2 employed here differ from those originally adopted in Ref. 3 (1.55 and 2.0, respectively). The value of c_2 quoted here is taken from Hanjalic and Launder[8] where it is deduced from the decay of high-Reynolds-number grid turbulence data. Since the production and dissipation rates of turbulence energy are nearly in balance in wall flows, the difference between the constants c_1 and c_2 is important. The value of c_1 used here is obtained by keeping this difference the same as that of Ref. 3. The usual boundary-layer approximations have been made in Eqs. (1) and (2) where D/Dt is the substantial derivative, x and y are, respectively, the coordinates parallel and normal to the solid wall, and u the velocity component in the x direction. The quantities k and ϵ are, respectively, the kinetic energy of turbulence and the "isotropic" dissipation (where the summation convention is adopted)

$$\epsilon = \nu\overline{\frac{\partial u_i'}{\partial x_j}\frac{\partial u_i'}{\partial x_j}} \tag{5}$$

which is not the true rate of energy dissipation[1]

$$D = \overline{\nu sij'\, sij'} \tag{6}$$

where $sij' = [(\partial u_i'/\partial x_j) + (\partial u_j'/\partial x_i)]/2$. At high Reynolds

numbers, $D=\epsilon$ because the small-scale turbulence is then isotropic.

To develop a model that will provide predictions of the flow down to the solid wall, the form of the model described in Eqs. (1-4) needs to be modified in several ways. Following Jones and Launder,[3] the kinematic viscosity is added to the turbulent diffusivity in Eqs. (1) and (2) to account for the molecular diffusion of k and ϵ, respectively. Furthermore, the dissipation term in Eq. (2) is modified to fit the data of the decaying homogeneous grid turbulence at both high and low Reynolds numbers, although the particular form used is that of Hanjalic and Launder.[8] The effect of the presence of the solid wall is handled differently. Consider a Taylor series expansion for the fluctuating velocity components near the wall, $y=0$. Because of the no-slip boundary condition and the continuity equation for an incompressible fluid, one obtains[7,9,10]

$$k\sim y^2 \tag{7}$$

$$\nu_t\sim y^3 \tag{8}$$

A Taylor series expansion of Eq. (2) near $y=0$ indicates that the "isotropic" dissipation

$$\epsilon\sim y^N \tag{9}$$

with the integer $N\geq 1$. Since the molecular diffusion of k is finite at $y=0$ as can be seen from Eq. (7), an additional term which represents the true finite rate of energy dissipation at the wall is needed to balance the molecular diffusion term. Substituting the Taylor series of the fluctuating velocity components into Eq. (6), one may obtain at $y=0$

$$D=2\nu k/y^2 \tag{10}$$

where ν is the kinematic viscosity. It is obvious from Eqs. (7) and (10) that D is indeed equal to the molecular diffusion at $y=0$. The right hand side of Eq. (10) will be termed the "wall" dissipation. It is assumed that the dissipation term in the turbulent kinetic energy equation at finite values of y is given by $\epsilon+(2\nu k/y^2)$. Therefore, the low-Reynolds-number form of Eq. (1) is written as follows

$$\frac{Dk}{Dt}=\frac{\partial}{\partial y}\left[(\nu+\nu_t)\frac{\partial k}{\partial y}\right]+\nu_t\left(\frac{\partial u}{\partial y}\right)^2-\epsilon-\frac{2\nu k}{y^2} \tag{11}$$

In essence, the low-Reynolds-number ϵ-equation of Jones and Launder[3] is equivalent to choosing the exponent N in Eq. (9) to be unity. Therefore, the dissipation term of the high-Reynolds-number ϵ-equation, being now finite at $y=0$, balances the molecular diffusion term at the wall. In addition, since the limiting form for ν_t as the direct effect of viscosity is negligible is given by Eq. (4), Eq. (8) is automatically satisfied. However, they found it necessary to add an empirical term (which vanishes at $y=0$) to the ϵ-equation and to multiply Eq. (4) by an empirical function (which varies between $e^{-2.5}$ at $y=0$ and 1 at high turbulence Reynolds numbers).

In the present paper, Eq. (4) is modified to include only the "damping" effect due to the presence of the solid wall

$$\nu_t=c_\mu(k^2/\epsilon)\left[1-\exp(-c_3u_*y/\nu)\right] \tag{12}$$

where u_* is the friction velocity and c_3 a constant. In addition, we note that the turbulence length scale $\sim k^{3/2}/\epsilon\sim y$ in the fully turbulent "logarithmic" region near a solid wall. This relation is assumed to hold even in the viscous sublayer so that Eq. (12) is consistent with Eq. (8). In other words, the exponent N in Eq. (9) is chosen to be 2. This is accomplished by adding in the high-Reynolds-number ϵ-equation a "wall" dissipation term that is similar in form to Eq. (10), namely, $(2\nu\epsilon/y^2)\exp[-(c_4u_*y/\nu)]$, where c_4 is another constant. Therefore, the low-Reynolds-number form of Eq. (2) is written in the following form:

$$\frac{D\epsilon}{Dt}=\frac{\partial}{\partial y}\left[\left(\nu+\frac{\nu_t}{\sigma}\right)\frac{\partial\epsilon}{\partial y}\right]+c_1\frac{\epsilon}{k}\nu_t\left(\frac{\partial u}{\partial y}\right)^2-\frac{\epsilon}{k}\left[c_2f\epsilon+\frac{2\nu k e^{-c_4u_*y/\nu}}{y^2}\right] \tag{13}$$

where[8]

$$f=1-\frac{0.4}{1.8}e^{-(k^2/6\nu\epsilon)^2} \tag{14}$$

Expanding the above equation near $y=0$, one may confirm that the behavior $\epsilon\sim y^2$ is achieved and the "wall" dissipation exactly balances the molecular diffusion at $y=0$.

In summary, our new model of turbulence is assumed to be governed by Eqs. (11-13) with two new constants c_3 and c_4. Before testing the present modeling and fixing the numerical values of c_3 and c_4 by considering the problem of a fully developed channel flow, we shall first briefly describe the numerical procedure employed.

Numerical Procedure

Each of the governing equations can be written in the following form:

$$a\frac{\partial f}{\partial x}+b\frac{\partial f}{\partial y}=\frac{\partial}{\partial y}\left(c\frac{\partial f}{\partial y}\right)+d+ef \tag{15}$$

For example, for Eq. (11) the choice of the coefficients can be

$$a=u \tag{16}$$

$$b=v \tag{17}$$

$$c=\nu+\nu_t \tag{18}$$

$$d=-\epsilon \tag{19a}$$

$$e=\frac{\nu_t}{k}\left(\frac{\partial u}{\partial y}\right)^2-\frac{2\nu}{y^2} \tag{20a}$$

Equation (15) is approximated by a second-order accurate, two-station, six-point central difference scheme. Conditions at the first x station are known and those at the second station Δx downstream are sought. The detailed equations can be found in Ref. 11. To better resolve the rapid variations occurring near the wall, a special nonuniform mesh distribution in the y direction is used which still allows us the usage of the central difference formulas for uniform mesh. This is accomplished by employing the procedure of using m_1 intervals of mesh size Δy starting from the wall, continued with m_2 intervals of mesh size $2\Delta y$, and then continued with m_3 intervals of mesh size $4\Delta y$, and so on. At the interface of different mesh sizes, say point m, the derivatives with respect to y are approximated by central finite-difference formulas using points $m-2$, m and $m+1$ and the corresponding mesh size. Typically, 8 such regions with a total number of more than 100 grid points are used. Growth of the boundary layer is allowed for by adding points in the y direction when needed.

Equations are decoupled and the coefficients of each difference equation are known during the iterative procedure so that the system of difference equations is in the tridiagonal form which can be solved very efficiently using the standard Gaussian two-step elimination procedure.[12] A complete

solution is obtained by iteration. Results at the previous x-station are used initially to start the calculation and the iterative procedure is continued until converged.

The diagonal dominance condition[12] of the tridiagonal system of difference equations may impose a condition on the mesh size in the x direction, Δx. As shown in Ref. 11, the crucial factor is the sign of the coefficients a and e of Eq. (15). For the problems considered in the present paper, there is no flow separation ($a=u>0$) and the diagonal dominance condition imposes a condition on the maximum Δx allowed

$$\Delta x \leq 2a/e \tag{21}$$

if $e>0$; but there is no restriction on Δx (assumed positive) if $e<0$.[11] Comparing Eqs. (13) and (15), it is obvious that the coefficient e for the ϵ-equation is always negative. Therefore, we need to concentrate on the k-equation only. From Eq. (20a), e is negative near the wall but becomes positive when energy production exceeds the "wall" dissipation. Since energy production reaches its maximum near the outer edge of the viscous sublayer and u increases monotonically in y, the minimum of the right hand side of Eq. (21) occurs in the outer portion of the viscous sublayer.

The corresponding choice of the coefficient e for the k-equation of Jones-Launder model is

$$e=\frac{\nu_t}{k}\left(\frac{\partial u}{\partial y}\right)^2-\frac{2\nu}{k}\left(\frac{\partial k^{1/2}}{\partial y}\right)^2 \tag{22a}$$

Clearly, its behavior is somewhat similar to Eq. (20a) of the present model. For the cases considered in the present paper, calculations indicate that the maximum value of Δx which satisfies the diagonal dominance condition across the whole boundary layer (henceforth denoted by Δx_m) of their model is about two-thirds of the present model.

It should be pointed out that the choice of the coefficients made above is not unique. In fact, a better choice can be made by noting that since the "wall" dissipation term in Eq. (11) and the corresponding term of Jones-Launder model are negative, the diagonal dominance condition is always satisfied if the production term is lagged behind during the iterations, i.e., by setting

$$d=\nu_t(\partial u/\partial y)^2-\epsilon \tag{19b}$$

For the present model, the term e is thus

$$e=-(2\nu/y^2) \tag{20b}$$

and for the Jones-Launder model, it becomes

$$e=-\frac{2\nu}{k}\left(\frac{\partial k^{1/2}}{\partial y}\right)^2 \tag{22b}$$

As shown in Ref. 11, these new choices of the coefficients of Eq. (15) have resulted in a large increase in Δx_m. Using an identical nonuniform mesh distribution as described before, this increase is a factor of 28 and 10 for the present and Jones-Launder models, respectively.

Fully Developed Channel Flow

Equations (11-13) have been applied to the study of turbulent flow between two parallel plates driven by a constant pressure gradient. The plates are separated by a distance $2H$ in the y direction and the mean flow is in the x direction. Therefore, the continuity equation is automatically satisfied and the momentum equation reduces to

$$(\nu+\nu_t)\frac{du}{dy}=u_*^2\frac{(H-y)}{H} \tag{23}$$

One may nondimensionalize the equations through the substitutions

$$\tilde{y}=y/H,\ \tilde{u}=u/u_*,\ \tilde{k}=k/u_*^2,\ \tilde{\epsilon}=\epsilon/(u_*^3/H),\ \tilde{\nu}_t=\nu_t/\nu$$

For convenience, the tilde notation is suppressed and it is understood that from now on all variables are dimensionless. Since k and ϵ depend only on y for a fully developed flow, the governing equations become

$$\frac{du}{dy}=Re^*\left(\frac{1-y}{1+\nu_t}\right) \tag{24}$$

$$\frac{d}{dy}\left[(1+\nu_t)\frac{dk}{dy}\right]+\nu_t\left(\frac{du}{dy}\right)^2-Re^*\epsilon-\frac{2k}{y^2}=0 \tag{25}$$

$$\frac{d}{dy}\left[\left(1+\frac{\nu_t}{\sigma}\right)\frac{d\epsilon}{dy}\right]+c_1\frac{\epsilon}{k}\nu_t\left(\frac{du}{dy}\right)^2-c_2Re^*f\frac{\epsilon^2}{k}$$
$$-\frac{2\epsilon}{y^2}\exp(-c_4Re^*y)=0 \tag{26}$$

$$\nu_t=c_\mu Re^*\frac{k^2}{\epsilon}[1-\exp(-c_3Re^*y)] \tag{27}$$

$$f=1-\frac{0.4}{1.8}\exp\left[-\left(\frac{Re^*k^2}{6\epsilon}\right)^2\right] \tag{28}$$

where $Re^*=u_*H/\nu$. The usual laboratory Reynolds number Re is based on the maximum mean velocity on the channel centerline and is related to Re^* by

$$Re=u(1)Re^* \tag{29}$$

At $y=0$, the boundary conditions are

$$u=k=\epsilon=0 \tag{30}$$

and at $y=1$,

$$\frac{dk}{dy}=\frac{d\epsilon}{dy}=0 \tag{31}$$

Of course, it is also required that k/ϵ be bounded at $y=0$.

The above set of equations was solved by the numerical procedure described before, with Eqs. (16) and (17) being replaced by $a=1$ and $b=0$. Calculations were continued in x until the final "steady-state" solutions were obtained. Results were found to be quite insensitive to the particular value of c_4 chosen. Therefore, $c_4=0.5$, which was used in our preliminary study,[10] is kept unchanged. The sensitivity of the predicted values to the choice of c_3 is more moderate. For example, for Re between 4100 and 30,800, a decrease of c_3 from 0.0115 to 0.01 has resulted in about 4% reduction in the skin friction c_f and about 5% increase in the peak turbulent kinetic energy. Its effect on other quantities is smaller.

The defect velocity based on $c_3=0.0115$ is shown in Fig. 1 for $Re=4100$ and 30,800. Also shown are the measurements of Laufer[13] at $Re=30,800$, of Clark[14] at a slightly higher Re ($=32,500$), and of Eckelmann[15] at $Re=4100$. When the data are plotted in this form, as one would expect the defect velocity distribution is indeed independent of Re in the major part of the flow that is not too close to the solid wall. Present theory is seen to agree with the data not only in this part of the flow, but also across the entire channel.

The turbulent shear stress distribution of the present prediction is compared with the measurements of Laufer[13] in Fig. 2 at $Re=12,300$ and 30,800. The agreement is again very good.

A more critical evaluation of the present model is a comparison of the turbulent kinetic energy distribution in the near-wall region. Such a comparison is best depicted using the

classical stretched nondimensional distance from wall y^+. In addition to the channel measurements of Refs. 13, 14, and 16, the pipe flow data of Laufer[17] and that of Schildknecht et al.[18] are also included in Fig. 3. The largest value of y^+ of the data of Ref. 18 used here corresponds to $(R-r)/R \approx 0.06$ (where R is the pipe radius and r the radial distance) where the curvature effect present in the pipe flow is expected to be small. Results of Ref. 16 are of high accuracy in the inner layer of the flow since measurements were made in an oil channel where a very thick viscous sublayer is produced. Also shown in Fig. 3 are the present predictions at $Re = 3850$, 15,200, and 30,800, respectively. Because of the large amount of scatter among all of the data, a definitive conclusion on the accuracy of the present theory is difficult to draw. The present model yields predictions that seem to capture the general shape and lie within the band of the data.

To provide a proper perspective, calculations based on the turbulence model of Jones and Launder[3] (JL) have also been carried out. The corresponding turbulent kinetic energy results are compared with the same set of experimental data in Fig. 4. It is clear that the degree of agreement here is worse than that shown in Fig. 3.

A more definitive evaluation of the present model in the near-wall region is provided in Fig. 5 where the present turbulent shear stress prediction is compared with the measurements of Laufer,[13,17] Eckelmann,[15] and Schildknecht et al.[18] Although more data at larger values of y^+ for $Re = 4100$ would be highly desirable, the predicted behavior of an essentially no Reynolds number effect at $y^+ \lesssim 10$ and the strong Reynolds number effect at larger values of y^+ is seen to be qualitatively and quantitatively verified by the data.

Turbulent Flow over a Flat Plate

Equations (11-13) with the same constants have also been applied to the problem of a turbulent boundary-layer flow over a flat plate. These equations and the continuity and the

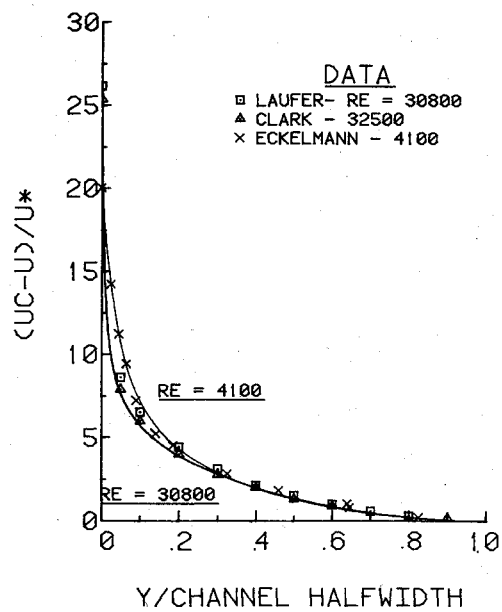

Fig. 1 Velocity distribution across the two-dimensional channel.

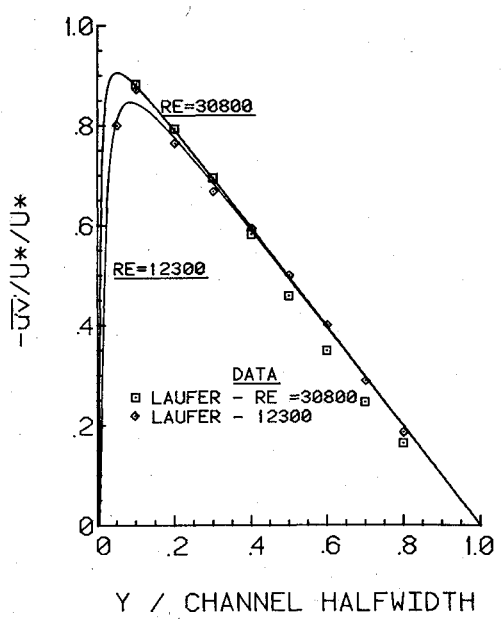

Fig. 2 Turbulent shear stress distribution across the channel.

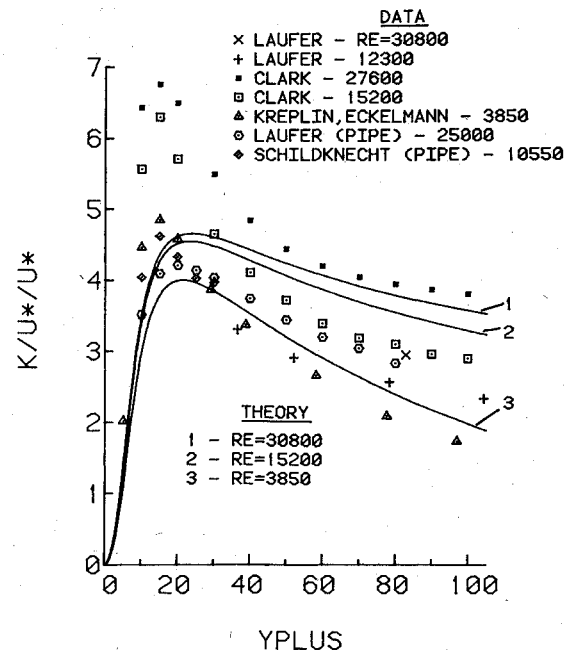

Fig. 3 Comparison of turbulent kinetic energy data near the channel wall with the present theory.

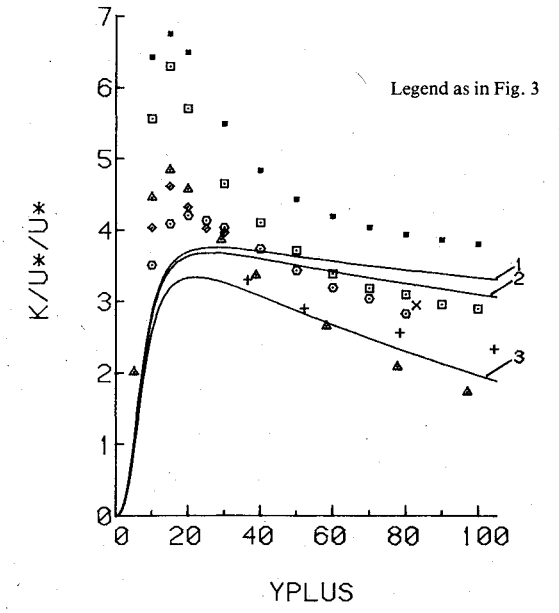

Fig. 4 Comparison of turbulent kinetic energy data near the channel wall with the theory of Jones and Launder.

momentum equations were solved by the same numerical procedure described before. The calculated distribution of the skin friction c_f as a function of the Reynolds number based on the momentum thickness $R_{e\theta}$ is compared with the measurements of Smith and Walker[19] and Wieghardt and Tillmann,[20] and with the correlation formulas of Coles[21] and Karman and Schoenherr[22] in Fig. 6. The agreement is seen to be extremely good.

The calculated nondimensional velocity $u^+(\equiv u/u_*)$ at $R_{e\theta}=7700$ is plotted against y^+ in Fig. 7. Also shown are the measurements of Klebanoff[23] at the same $R_{e\theta}$ and those of Wieghardt and Tillmann[20] at $R_{e\theta}=7170$ and 8170, respectively. It is clear from Fig. 7 that the agreement is very good.

The distribution of the turbulent kinetic energy (normalized by the freestream velocity squared) across the flat-plate boundary layer as predicted by the present model at $R_{e\theta}=7700$ is compared in Fig. 8 with Klebanoff's data[23] at the same Reynolds number ($y=0$ is at the wall and $y/\delta=1$ is at the boundary-layer edge). The theory predicts a very sharp increase of the turbulent kinetic energy from zero at the wall to a peak at $y/\delta\approx 0.0089$, and then an almost equally rapid drop followed by a much slower decline. Although Klebanoff's data do not locate the peak exactly, the agreement with the theory is very good.

Calculations using the same numerical scheme but based on the JL model[3] have also been carried out. To reduce the computational cost, the results of the JL model shown here have been started at $R_{e\theta}=5250$ using the results of the present model at that location as the initial conditions. The influence of the initial conditions died down rather quickly and the calculated c_f distribution is also included in Fig. 6. It is seen that the agreement is quite good, although the JL model yields a prediction that is slightly lower than the data and the present theory. The calculated u^+ distribution at $R_{e\theta}=7700$ based on the JL model, as shown in Fig. 7, is in good agreement with the present model and with the data. On the other hand, similar to the channel flow results, the turbulent kinetic energy distribution of the JL model as shown in Fig. 8 is seen to yield a peak value that is considerably lower than both the measurements and the present theory.

Conclusion

A turbulence model that is valid down to a solid wall has been developed and applied to the channel flow and boundary-layer flow. Comparisons between the present theory and the various experimental measurements have been made and good agreement has been found in general. Calculations based on the Jones-Launder model indicate that its prediction

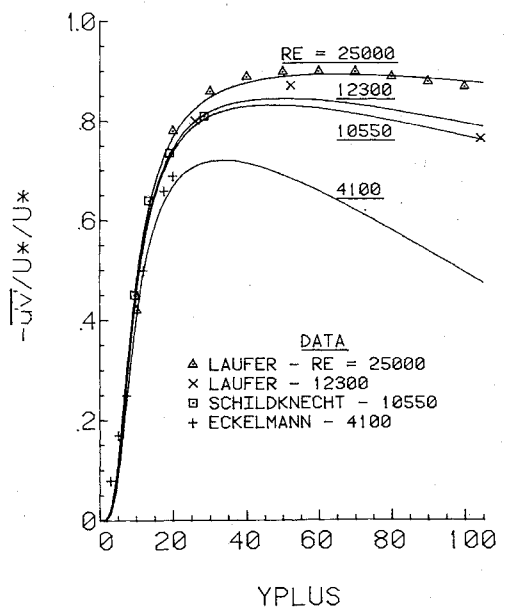

Fig. 5 Turbulent shear stress distribution near the channel wall.

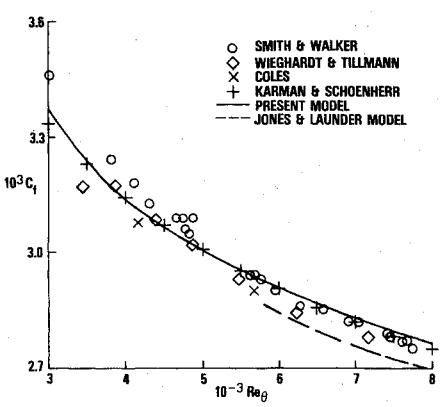

Fig. 6 Flat-plate skin friction distribution.

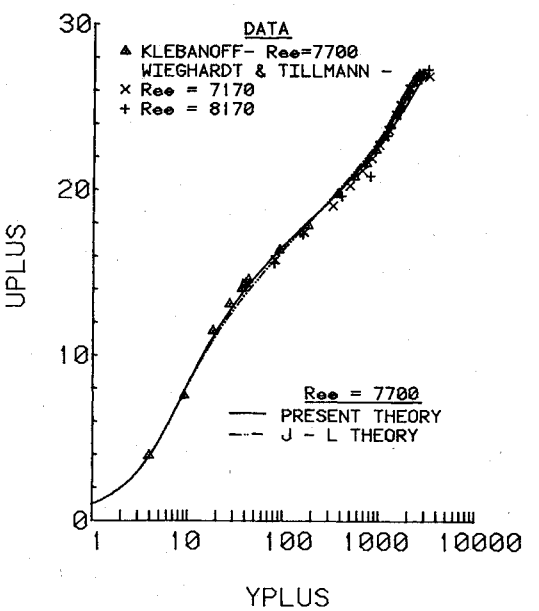

Fig. 7 Velocity distribution across the boundary layer.

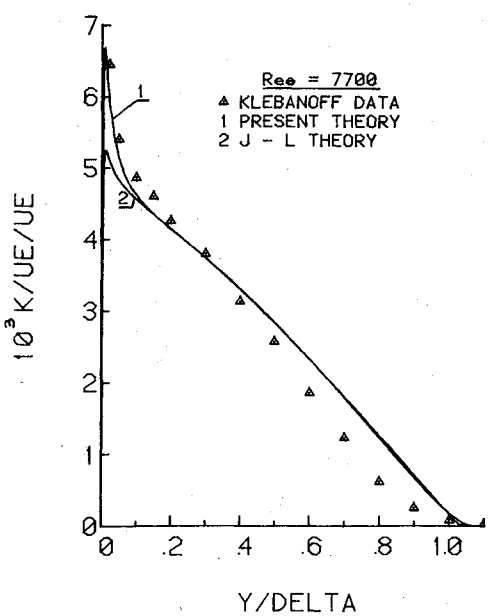

Fig. 8 Turbulent kinetic energy distribution across the boundary layer.

of the peak turbulent kinetic energy and its numerical efficiency are inferior to the present model.

Acknowledgment

This work was sponsored by the Naval Air Systems Command, Task 9R02302003 (Boundary Layer Research) under the cognizance of W. C. Volz (AIR 320C) and by the NSWC Independent Research Program.

References

[1] Reynolds, W. C., "Computation of Turbulent Flows," *Annual Review of Fluid Mechanics,* Vol. 8, 1976, pp. 183-208.

[2] Ng, K. H. and Spalding, D. B., "Turbulence Model for Boundary Layers Near Walls," *Physics of Fluids,* Vol. 15, Jan. 1972, pp. 20-30.

[3] Jones, W. P. and Launder, B. E., "The Prediction of Laminarization with a 2-Equation Model of Turbulence," *International Journal of Heat and Mass Transfer,* Vol. 15, Feb. 1972, pp. 301-314.

[4] Saffman, P. G. and Wilcox, D. C., "Turbulent Model Predictions for Turbulent Boundary Layers," *AIAA Journal,* Vol. 12, April 1974, pp. 541-546.

[5] Vollmers, H. and Rotta, J. C., "Similar Solutions of the Mean Velocity, Turbulent Energy and Length Scale Equation," *AIAA Journal,* Vol. 15, May 1977, pp. 714-720.

[6] Glushko, G. S., "Turbulent Boundary Layer on a Flat Plate in an Incompressible Fluid," NASA TT F-10080, 1965.

[7] Mellor, G. L. and Herring, H. J., "A Survey of the Mean Turbulent Field Closure Models," *AIAA Journal,* Vol. 11, May 1973, pp. 590-599.

[8] Hanjalic, K. and Launder, B. E., "Contribution Towards a Reynolds-Stress Closure for Low-Reynolds-Number Turbulence," *Journal of Fluid Mechanics,* Vol. 74, April 1976, pp. 593-610.

[9] Reichardt, H., "Vollstandige Darstellung der turbulenten Geschwindigkeitsverteilung in glatten Leitungen," *Zeitschrift fur Angewandte Mathematik und Mechanik,* Vol. 31, July 1951, pp. 208-219.

[10] Chien, K.-Y., "On the Modeling of Turbulence Near a Solid Wall," Paper presented at Navy/Air Force Science and Engineering Symposium, San Diego, Calif., Oct. 1978.

[11] Chien, K.-Y., "On the Numerical Convergence and Efficiency of Two Low-Reynolds-Number Turbulence Model Equations," *Proceedings of the 6th US-FRG Data Exchange Agreement Meeting on Viscous and Interacting Flow Field Effects,* DFVLR-AVA, Göttingen, West Germany, April 1981, to be published.

[12] Isaacson, E. and Keller, H. B., *Analysis of Numerical Methods,* John Wiley & Sons, New York, 1966, pp. 55-57.

[13] Laufer, J., "Investigation of Turbulent Flow in a Two-Dimensional Channel," NACA Rept. 1053, 1951.

[14] Clark, J. A., "A Study of Incompressible Turbulent Boundary Layers in Channel Flow," *Journal of Basic Engineering,* Vol. 90, Dec. 1968, pp. 455-468.

[15] Eckelmann, H., "The Structure of the Viscous Sublayer and the Adjacent Wall Region in a Turbulent Channel Flow," *Journal of Fluid Mechanics,* Vol. 65, Pt. 3, Sept. 1974, pp. 439-459.

[16] Kreplin, H.-P. and Eckelmann, H., "Behavior of the Three Fluctuating Velocity Components in the Wall Region of a Turbulent Channel Flow," *Physics of Fluids,* Vol. 22, July 1979, pp. 1233-1239.

[17] Laufer, J., "The Structure of Turbulence in Fully Developed Pipe Flow," NACA Rept. 1174, 1954.

[18] Schildknecht, M., Miller, J. A., and Meier, G. E. A., "The Influence of Suction on the Structure of Turbulence in Fully Developed Pipe Flow," *Journal of Fluid Mechanics,* Vol. 90, Pt. 1, Jan. 1979, pp. 67-107.

[19] Smith, D. W. and Walker, J. H., "Skin-Friction Measurements in Incompressible Flow," NASA TR R-26, 1959.

[20] Wieghardt, K. and Tillmann, W., "On the Turbulent Friction Layer for Rising Pressure," NACA TM 1314, 1951.

[21] Coles, D. E., "The Turbulent Boundary Layer in a Compressible Fluid," The Rand Corp., Rept. R-403-PR, 1962.

[22] Hopkins, E. J. and Inouye, M., "An Evaluation of Theories for Predicting Turbulent Skin Friction and Heat Transfer on Flat Plates at Supersonic and Hypersonic Mach Numbers," *AIAA Journal,* Vol. 9, June 1971, pp. 993-1003.

[23] Klebanoff, P. S., "Characteristics of Turbulence in a Boundary Layer with Zero Pressure Gradient," NACA Rept. 1247, 1955.